Quantifying the potential for reservoirs to secure future surface water yields in the world's largest river basins

Lu Liu[1,2*], Simon Parkinson[2,3], Matthew Gidden[2], Edward Byers[2], Yusuke Satoh[2], Keywan Riahi[2], and Barton Forman[1]

1. Department of Civil and Environmental Engineering, University of Maryland, College Park, MD, USA
2. International Institute for Applied Systems Analysis, Laxenburg, Austria
3. Institute for Integrated Energy Systems, University of Victoria, Victoria, BC, Canada

Abstract

Surface water reservoirs provide us with reliable water supply, hydropower generation, flood control and recreation services. Yet, reservoirs also cause flow fragmentation in rivers and lead to flooding of upstream areas, thereby displacing existing land-use activities and ecosystems. Anticipated population growth and development coupled with climate change in many regions of the globe suggests a critical need to assess the potential for future reservoir capacity to help balance rising water demands with long-term water availability. Here, we assess the potential of large-scale reservoirs to provide reliable surface water yields while also considering environmental flows within 235 of the world's largest river basins. Maps of existing cropland and habitat conservation zones are integrated with spatially-explicit population and urbanization projections from the Shared Socioeconomic Pathways (SSP) to identify regions unsuitable for increasing water supply by exploiting new reservoir storage. Results show that even when maximizing the global reservoir storage to its potential limit (~4.3-4.8 times the current capacity), firm yields would only increase by about 50% over current levels. However, there exist large disparities across different basins. The majority of river basins in North America are found to gain relatively little firm yield by increasing storage capacity, whereas basins in Southeast Asia display greater potential for expansion as well as proportional gains in firm yield under multiple uncertainties. Parts of Europe, the

United States and South America show relatively low reliability of maintaining current firm yields under future climate change, whereas most of Asia and higher latitude regions display comparatively high reliability. Findings from this study highlight the importance of incorporating different factors, including human development, land-use activities, and climate change, over a time span of multiple decades and across a range of different scenarios when quantifying available surface water yields and the potential for reservoir expansion.

1. Introduction

Surface water reservoirs help dampen flow variability in rivers while playing a critical role in flood mitigation, securing water supplies, and ensuring reliable hydropower generation. In 2011, total global storage capacity of the largest reservoirs was approximately 6197 km^3 and affected the flow in almost half of all major river systems worldwide (Lehner et al., 2011). Changes in natural flow patterns can disrupt local ecosystems (Poff and Schmidt, 2016; Richter et al., 2012), and inundation of upstream areas during reservoir development can cause conflicts with existing land-uses (Richter et al., 2010). Reservoirs also require a significant amount of resources to plan, build and operate, with implications for long-term water supply costs and affordability (Wiberg and Strzepek, 2005). Quantifying exploitable reservoir capacity is therefore crucial for strategic planning of water, energy and food supplies in the coming decades, particularly with anticipated population growth and exacerbating impacts on hydrological variability due to climate change (Boehlert et al., 2015; Kundzewicz and Stakhiv, 2010; Soundharajan et al., 2016; Stillwell and Webber, 2013; Vörösmarty et al., 2009).

Storage-yield (S-Y) analysis is often used by water resource planners to determine the reservoir storage capacity required to provide firm yield (Rippl, 1883; Turner and Galelli, 2016). The firm yield represents the maximum volume of water that can be supplied from the reservoir for human purposes (e.g., irrigation, municipal supply, etc.) under a stated reliability. A number of previous studies evaluate different algorithms for modeling the S-Y relationship (Carty and Cunnane, 1990), and have included storage-dependent losses (Lele, 1987) and generalized functional forms for broader scale application (Kuria and Vogel, 2015; Vogel et al., 2007; Vogel and Stedinger, 1987). For example, *McMahon et al.* (2007) developed six empirical equations to calculate reservoir capacities for 729 unregulated rivers around the world. A number of other previous studies employ S-Y algorithms to provide insight into various water security challenges moving forward. *Wiberg and Strzepek* (2005) developed S-Y relationships and associated costs for major watershed regions in China accounting for the effects of climate change. Similarly, *Boehlert et al.* (2015) computed S-Y curves for 126 major basins globally under a diverse range of climate models and scenarios to estimate the potential scale of adaptation measures required to maintain surface water supply reliability. *Gaupp et al.* (2015) calculated S-Y curves for 403 large-scale river basins to examine how existing storage capacity can help manage flow variability and transboundary issues. Basin scale S-Y analysis provides estimates on hypothetical storage capacity required to meet water demand, and hence, such analysis helps to identify the need for further infrastructure investments to cope with water stress on a global scale (Gaupp et al., 2015). Even though previous analyses of both global and regional energy systems suggest that evaporative losses from reservoirs used for hydropower play a significant role in total consumptive water use (Fricko et al., 2016; Grubert, 2016), such evaporative impacts are missing from existing global-scale assessments of surface water reservoir potential that consider climate change. Increasing air temperatures and variable regional precipitation patterns associated with climate change will ultimately affect evaporation rates. Moreover, competing land-uses and environmental flow regulations play an important role in large-scale reservoir siting and operations, but have yet to be considered concurrently as part of a global-scale assessment of the ability of future reservoirs to provide sustainable firm yields under climate change. Additional constraints on reservoir operation and siting will reduce firm yields, but these effects could be offset in basins where runoff is projected to increase under climate warming (van Vliet et al., 2016). Development of new, long-term systems analytical tools to disentangle the tradeoffs between potential reservoir firm yield, climate change, and competing land-use options is therefore a critical issue to address from the perspective of water resources planning.

The purpose of this study is to assess the aggregate potential for reservoirs to provide surface water yields in 235 of the world's largest river basins, including consideration of climate change impacts on basin-wide runoff and net evaporation (i.e., the difference between estimated evaporation from the reservoir surface and the incident precipitation), as well as constraints on reservoir development and operation due to competing land-uses and environmental flow requirements. Improved basin-scale S-Y analysis tools enabling global investigation are developed for this task, including a linear programming (LP) framework that contains a reduced-form representation of reservoir evaporation and environmental flow allocation as endogenous decision variables. The framework incorporates additional reservoir development constraints from population growth, human migration, existing irrigated cropland, and natural protected areas. We further consider a range of future global change scenarios and measure reservoir performance in terms of yield and corresponding reliability as to maintain a given yield across global change scenarios. The scope of this analysis thus covers a number of important drivers of water supply sustainability neglected in previous global assessments while also providing new insight into the following research questions:

- In which basins are surface water withdrawals from reservoirs most affected by future climate change? And how might achieving climate change mitigation targets limit such impact?

- What are the impacts of competing land-use activities and environmental flow constraints on the potential of expanded reservoirs to secure freshwater yields?

2. Methodology

This study assesses aggregate reservoir storage potential and surface water firm yields at the river basin-scale. River basins represent the geographic area covering all land where any runoff generated is directed towards a single outlet (river) to the sea or an inland sink (lake). The approach builds on previous work that combines basin-averaged, monthly runoff data with a simplified reservoir representation to derive the S-Y relationships for different basins in a computationally efficient way (Wiberg and Strzepek 2005; Boehlert et al. 2015; Gaupp et al., 2015). *Wiberg and Strzepek* (2005) tested a similar basin-scale approach to S-Y analysis using a number of simplified geometries for cascaded reservoir systems in the Southwest United States and showed relatively good agreement with management strategies simulated with a more complicated model. The resulting basin-scale S-Y relationships quantify the storage capacity needed to achieve a specified firm yield but do not prescribe locations for reservoirs within each river basin, which would require location-specific S-Y analysis. The basin-scale S-Y relationships provide a metric for understanding how changes in precipitation, evaporation, and land-use across space and time translate into changes in required storage needed at the basin-level to ensure a specified volume of freshwater is available for human use (e.g., irrigation, municipal supply, etc.). The basin-level S-Y indicators enable comparison across regions, and hence, identification of basins with the greatest challenges in terms of adapting to future climate change (Wiberg and Strzepek 2005; Boehlert et al. 2015).

A linear programming (LP) model computes the S-Y characteristics (section 2.2) and is applied to the 235 basins delineated in HydroSHEDS used by the Food and Agriculture

Organization of the United Nations (FAO) (http://www.fao.org/geonetwork/srv/en/metadata.show?id=38047). The LP model calculates the minimum reservoir capacity required to provide a given yield based on concurrent 30-year average monthly runoff sequences within each basin. This timeframe is selected to mimic existing regional water resource planning practices, which typically take a multi-decadal perspective to include analysis of long-lived infrastructure investments such as reservoir development (Gaupp et al., 2015).

Return of extracted groundwater to rivers and long-distance inter-basin transfers via conveyance infrastructure are important parts of the surface water balance in some regions (McDonald et al., 2014; Wada et al., 2016), but are not included in this current study due to lack of consistent observational data on a global scale and computational challenges preventing application of the LP framework at higher spatial resolutions. The approach also does not consider streamflow routing within basins. Omitting routing in basin-scale S-Y analysis has been adopted in previous studies (Gaupp et al., 2015). It is also important to note that in some of the largest basins the hydraulic residence time is on the order of several months, and hence, our analysis is unable to reflect the effects of this time-lag on storage reliability. Similarly, our assessment is unable to address capacity decisions focused on addressing floods, which usually requires assessing flow patterns at higher frequencies (Naden, 1992).

In this study, we assume an upper boundary for the maximum reservoir expansion scenario which is defined by the limited availability of land to be flooded due to various restrictions. Availability of land is defined following a spatially-explicit analysis of existing and future land-use in each basin (section 2.3). It is important to emphasize that additional reservoir development constraints not readily quantifiable with existing methods (e.g., soil stability, future habitat conservation, cultural preferences, etc.) are likely to further reduce available area for reservoir expansion.

The overall approach of the global scale assessment is shown in Figure 1. The historical period of 1971-2000 and a simulation period of 2006-2099 were analyzed for each of the 235 basins. The 30-year monthly runoff sequences were generated for each decade resulting in 8 decadal runoff sequences for each climate scenario. Additionally, the impacts of net evaporative losses from the reservoir surface are estimated for each climate scenario and included in the reservoir capacity calculations.

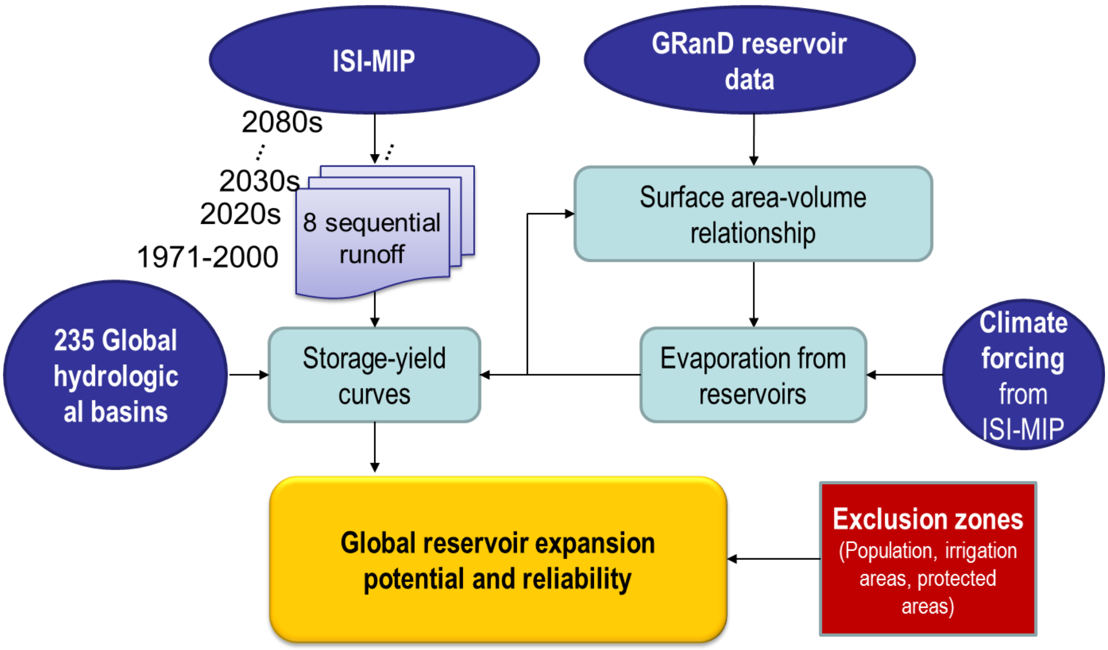

Figure 1. Framework for assessing impacts of climate change and human development constraints on the reservoir potential in 235 large-scale river basins.

2.1 Model inputs

For this study, we utilized runoff from a state-of-the-art global hydrological model (GHM) entitled PCR-GLOBWB (Wada et al., 2014). Similarly, we used climate inputs from an advanced general circulation model (GCM) entitled HadGEM2-ES (Jones et al., 2011), provided by the Inter-Sectoral Impact Model Intercomparison Project (ISI-MIP) Fast Track

(Hempel et al., 2013). PCR-GLOBWB estimates of daily runoff are, to the first-order, driven by climate inputs from bias-corrected HadGEM2-ES (Hempel et al., 2013). The GHM is well-validated over most of the large rivers at both monthly and daily time scales (van Beek et al., 2012, 2011). Hydrologic outputs from the GHM driven by a GCM have been applied in global scale studies (Schewe et al., 2014; Veldkamp et al., 2016; Wanders et al., 2015). In this study, the monthly runoff statistics are given based on daily runoff.

Similarly, net evaporative loss from the reservoir is forced by climate input from the GCM using the general approach of Shuttleworth (1993) (Appendix A section 2). This approach originated from the Penman equation (Penman, 1948) and is widely used to estimate the potential evaporation of open water and fully-saturated land surfaces (Harwell, 2012). Net evaporation is therefore the difference between estimated potential evaporation from reservoir surface and precipitation on reservoir surface.

All model inputs are provided as gridded data at 0.5-degree spatial resolution (approximately 50 km by 50 km in the mid-latitudes). Data for each of the four future climate change scenarios from the Representative Concentration Pathways (RCPs) (van Vuuren et al., 2011) are available. The four RCPs (2.6, 4.5, 6.0 and 8.5) describe a possible range of radiative forcing values by the year 2100 relative to pre-industrial values, which are consistent with a wide range of possible changes in global climate patterns. For example, the RCP2.6 scenario represents a low-carbon development pathway consistent with limiting the global mean temperature increase to 2 degrees C by 2100 (van Vuuren et al., 2011). Conversely, RCP8.5 represents a world with high population, energy demand, and fossil intensity, and thus the highest carbon emissions (Riahi et al., 2011). The inclusion of different global emission scenarios in the S-Y analysis provides insight into the potential interactions with climate change mitigation policy.

Similar to previous research, a simplified geometry for the representative reservoir in each basin is assumed (Wiberg and Strzepek 2005; Boehlert et al. 2015; Gaupp et al., 2015) (Appendix A section 1). The simplification is crucial in the current study for facilitating the long-term global-scale perspective needed to assess impacts of climate change across multiple scenarios. The Global Reservoir and Dam (GRanD) database (Lehner et al., 2011) reports the maximum storage capacity and surface area for existing reservoirs with a storage capacity of more than 0.1 km^3. These data are used to derive an average surface area-volume relationship for each basin (Appendix A section 1).

2.2 Reservoir storage-yield relationship

Reservoir capacity is defined in this study as the minimum storage capacity c capable of providing a firm yield y across a set of N discrete decision-making intervals, $\mathrm{T} = \{t_1, \dots, t_{\mathrm{N}}\}$. Considering average monthly runoff q, releases for environmental purposes r and net evaporative losses v, a simple water balance across basin-wide inflows and managed outflows at the representative basin reservoir results in the following continuity equation for the storage level:

$$s_{t+1} = s_t + q_t - v_t - r_t - y \;\forall\; t \in \{t_1, \dots, t_{N-1}\} \quad (1)$$

where s is the storage level. Evaporation and precipitation are important processes to parameterize in the reservoir water balance due to the feedback with management strategies (Wiberg and Strzepek, 2005). Level-dependent net evaporative losses are estimated assuming a linearized relationship between surface area and storage level (Lele, 1987):

$$v_t = e_t \cdot A_t = \frac{1}{2} \cdot e_t \cdot a \cdot (s_t + s_{t+1}) = \alpha_t \cdot (s_t + s_{t+1}) \;\forall\; t \in T \quad (2)$$

where e is the net evaporation (as equivalent depth), A is the reservoir surface area, a is the surface area per unit storage volume (Appendix A section 2), and $\alpha = 1/2 \cdot e \cdot a$. The net evaporation and reservoir geometry parameters represent basin-averages.

Combining (1) and (2) generates a continuity equation for the reservoir storage level that incorporates level-dependent net evaporative losses in a simplified way (Appendix A section 1). The continuity equation is joined with a number of operational constraints to form the following LP model:

$$\textbf{Min} \quad c \tag{3a}$$

$$\textbf{s.t.} \quad (1-\alpha_t)\cdot s_t - (1+\alpha_t)\cdot s_{t+1} - r_t = y - q_t \; \forall \, t \in \{t_1, \ldots, t_{N-1}\} \tag{3b}$$

$$s_{t_1} \leq s_{t_N} \tag{3c}$$

$$\rho \cdot c \leq s_t \leq \varphi \cdot c \; \forall \, t \in T \tag{3d}$$

$$r_{min} \leq r_t \leq r_{max} \; \forall \, t \in T \tag{3e}$$

$$0 \leq c \leq c_{max} \tag{3f}$$

where the management variables are defined by the set $\mathrm{X} = \{s, r, c\}$. The objective function (3a) seeks to minimize the no-failure storage capacity given a certain firm yield. Constraint (3b) is the continuity equation incorporating level-dependent net evaporative losses. Constraint (3c) prevents pre-filling and draining of the reservoir in the model by ensuring the storage level at the final time-step, t_N , does not exceed the storage level at the initial time step, t_1 . Constraint (3d) ensures the reservoir storage level stays within a maximum fraction of storage capacity, φ (assumed to be 1), and a minimum dead-storage limit of the installed capacity, ρ. Gaupp et al. (2015) adopted ρ of 20% in their study and this value can be as high as 30%-40% (Wiberg and Strzepek, 2005). In this study, we assumed a smaller fraction of 15%.

Constraint (3e) ensures the release is maintained between the maximum and minimum environmental flow requirements, r_{min} and r_{max}, which are computed by applying an augmentation factor on monthly natural streamflow. We adopted the environmental flow approach of Richter et al. (2012) where the environmental flow allocation is determined by an allowable augmentation from presumed naturalized conditions. We experimented with an augmentation factor of 10%-90% of the naturalized conditions. Results are shown with an augmentation factor of 90%, which serves as a lower bound for illustrative purposes. Hence, r_{min} and r_{max} is 10% and 190% of monthly natural streamflow, respectively. Constraint (3f) limits installed storage capacity to c_{max} and ensures the capacity remains positive. The maximum volume is set based on an assessment of within-basin land-use, which is further discussed in section 2.3.

Solving (3) identifies the minimum storage capacity required to provide the given firm yield subject to the operational constraints. The S-Y relationship is obtained by solving the model for incrementally increasing firm yields. From the S-Y curve, the maximum storage capacity for the reservoir within each basin occurs at the maximum firm yield, i.e., where the marginal gains in firm yield under reservoir expansion approach zero. Maximum reservoir storage potential is therefore equivalent to the maximum storage capacity derived from the S-Y relationship unless such storage capacity is constrained by available land, which is explained in section 2.3. The maximum gain in firm yield is thus the difference between the current firm yield and the maximum firm yield identified from the generated S-Y curve.

An ensemble of S-Y curves is generated for each basin using the climate scenarios and multi-decadal simulations described in section 2.1. The ensemble is assessed to calculate the number of S-Y curves in each basin that reach a given firm yield. This analysis provides an additional reliability-based performance metric that incorporates a measure of climate change uncertainty. Note that to accurately represent the reliability of reservoirs, behaviour simulation of reservoirs with assumptions of operating policy should be implemented (Kuria and Vogel, 2015). However, given the computational intensity of behaviour analysis, the reliability in this study represents the probability a certain firm yield can be obtained across the climate scenarios and multi-decadal planning horizons. That is, we assessed reliability in terms of reservoir potential and firm yields across different climate scenarios and decision-making periods.

2.3 Exclusion zones

Reservoir expansion, and the associated gains in firm yield, are constrained by the availability of land since not all areas can realistically be used for reservoir expansion. c_{max} in equation 3g is derived for each basin by calculating the storage volume associated with the total available land area (see Appendix A section 1). We followed the approach of a number of previous studies on renewable energy potentials (de Vries et al., 2007; Zhou et al., 2015) and define reservoir exclusion zones using maps of the following drivers: 1) population (Jones et al., 2016); 2) irrigated cropland (Siebert et al., 2013); and 3) protected areas (Figure S1 and Table S1) (Deguignet et al., 2014). We adopted dynamic population trajectories under two Shared Socioeconomic Pathways (SSPs) — SSP1 and SSP3. These scenarios were selected due to their opposing storylines about population growth and urbanization, which introduces human migration uncertainties into the analysis. SSP1 describes a future world with high urbanization and low population growth whereas lower urbanization and higher population growth define SSP3 (O'Neill et al., 2014). Total available land area for reservoir expansion in each basin is thus the remaining area outside the exclusion zones. Further discussion of the exclusions zones and the derivation is provided in Appendix A section 3.

Other than population, agriculture, and protected land, other physical limitations such as elevation, slope and seismic risk will also constrain the available area for reservoir expansions. It is important to further emphasize that this work does not prescribe actual sites for new reservoirs within basins, which requires a more detailed treatment of the local geography and stakeholder needs. Non-physical constraints such as economic incentives, institutional capacity, and infrastructure readiness would also limit the ability of reservoir capacity expansion. To fully characterize exclusion zones, future work should consider direct use of high-resolution digital elevation model data and alternative metrics for limiting land availability. Without considering non-physical constraints that are difficult to quantify, this study serves as a first-order estimation of reservoir storage and surface water yield expansion potential at global scale.

3 Results

Figure 2 depicts the combined impacts of climate change and competing land-use activities on reservoir storage potential and reliability in the 2050s under a maximum reservoir expansion scenario. There are two layers of information embedded in Figure 2: Storage expansion potential (vertical color) and the likelihood of maintaining current firm yields under future climate change (horizontal color). There are large disparities in the potential for reservoir expansion to provide firm yields across basins. For example, the majority of basins in Europe display greater than 2500m^3 of storage potential per capita, but relatively low reliability (<50%) for maintaining current firm yields due to the projected lower water availability under climate change. Basins in Asia show high reliability (>50%) for maintaining current firm yield yet relatively low storage potential (<2500 m^3) per capita associated with large projections in population growth. Basins located at higher latitudes generally display abundant storage potential (>12000m^3/capita), but these regions are not usually highly populated or water demanding; hence, there will likely be less of an incentive to plan for reservoir expansion in these regions. To quantify the necessity of building reservoirs to relieve regional water stress, it is necessary to integrate water demand from different sectors into this framework so that the reservoir expansion planning will take into account the severity of water scarcity as well as environmental and socioeconomic development factors.

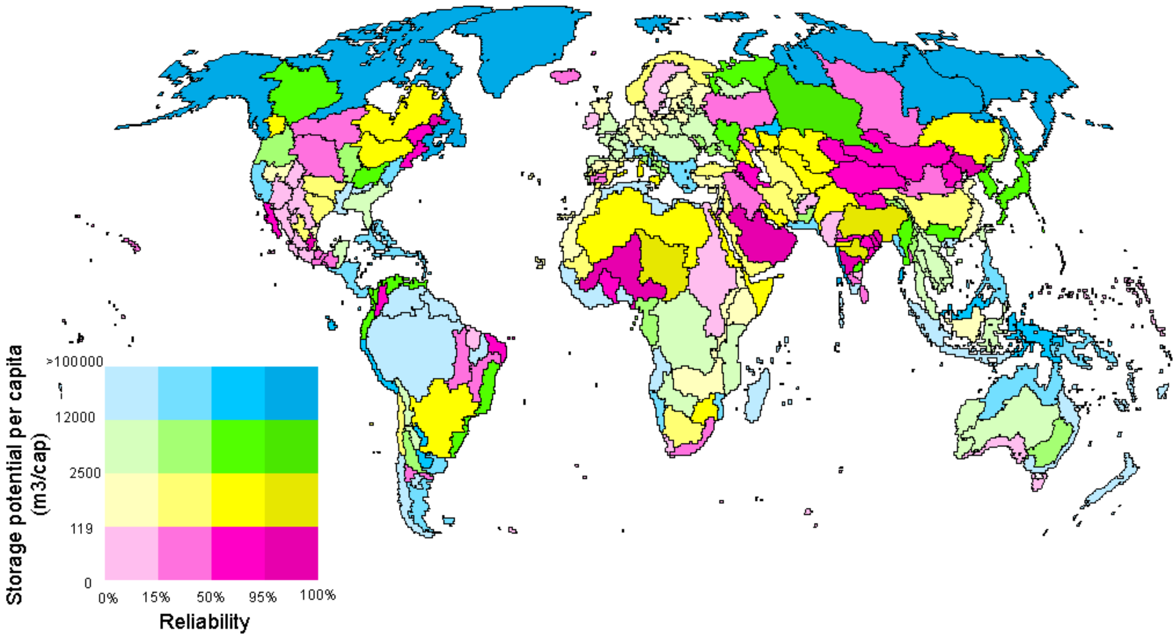

Figure 2. Bivariate map showing reliability (with respect to current firm yields) and maximum storage potential per capita by basin under SSP1 population trajectory in the 2050s

Maximizing the additional amount of reservoir storage (~4.3-4.8 times greater) results in only a ~50% increase in firm yield worldwide due to the nonlinear shape of the S-Y curve (ex. Figure S3 and S4). Figure 3 shows the marginal gains vary substantially across basins. Gains in storage/firm yield are defined as the ratio between estimated maximum reservoir storage/firm yield and current reservoir storage/firm yield and are computed by analyzing the S-Y curve for each basin of interest. The majority of basins in North America have limited gain in firm yield by maximizing storage as these basins have already been highly developed. Basins in parts of India and Southeast Asia, on the other hand, display relatively greater marginal gain in firm yield by maximizing storage capacity.

By comparing the two types of map products in Figure 2 and Figure 3, we can identify regions where reservoir expansion will be particularly challenging. For example, current total reservoir storage capacity in the Missouri River Basin, U.S. is 133 km^3. There is very little room for further expansion for the Missouri River Basin as the estimated storage potential is almost identical with current reservoir storage (Figure S3). Fully utilizing potential storage leads to negligible increases in firm yield, and with a reliability of less than 50% due to the relative instability of future water availability under the tested scenarios (Figure S2). In Asia, current total storage capacity in the Mekong Basin is 19 km^3, and the storage potential is about 300 km^3 (~16 times current storage) (Figure S3b). In contrast, additional storage per capita for the Mekong Basin is 4200 m^3/capita. By maximizing the potential storage, firm yield increases from 235 km^3 to ~500 km^3, which is approximately 2 times the current firm yield. However, the reliability is estimated to be very low due to the projected lower reservoir inflows under climate change (Figure S2). As Figure 2 and Figure 3 illustrate, there exists large regional heterogeneity in marginal gain of firm yield when we fully utilize potential storage and the reliability of maintaining current firm yield varies from basin to basin. In addition to physical feasibility, there are other factors that constrain storage potential and hence gain in firm yield. Additional global maps are included in Supplementary section to help understand current yields for each basin (Figure S7) and additional storage needed to maintain current firm yields (Figure S8).

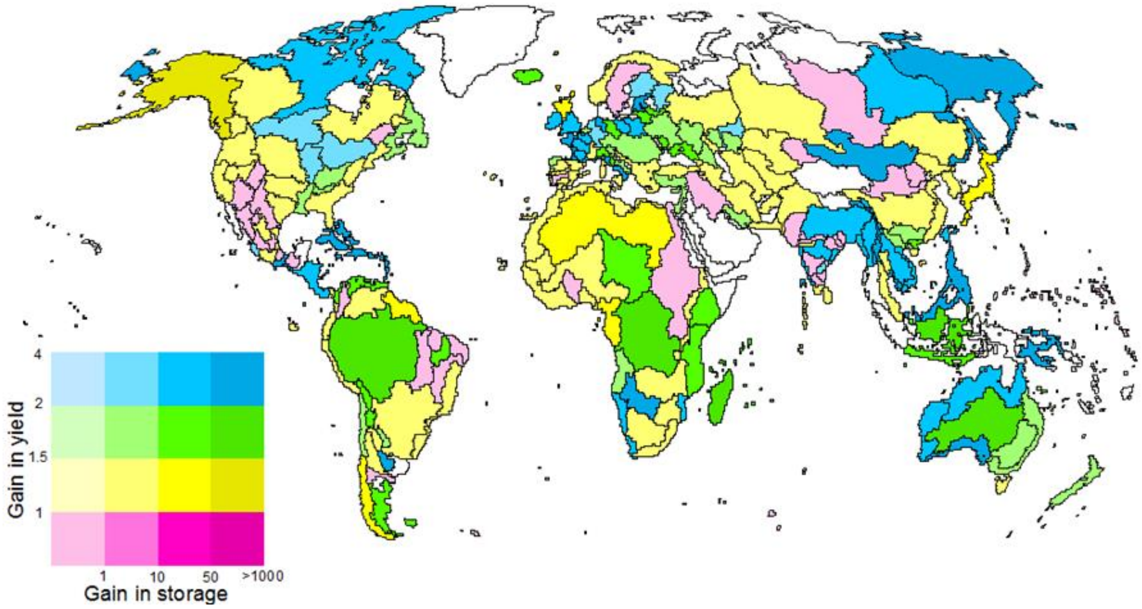

Figure 3. Bivariate map showing gains in firm yield/storage (unitless) for each basin under the SSP1 population trajectory in the 2050s (blank regions indicate insufficient GRanD data)

In this study, we experimented with different augmentation factors for environmental flow to show how many basins have already installed a storage capacity that exceeds presumed environmental guidelines. Table 1 shows the percentage of basins that would be overdeveloped if higher environmental flow requirements were assumed.

Table 1 Percentage of basins overdeveloped with respect to environmental flow requirements

Environmental flow requirements (% of natural streamflow)	Percentage of basins overdeveloped (%)
10%	7
20%	11
50%	20
70%	98
90%	98

Results suggest that even at "poor or minimum" environmental flow condition (Tennant, 1976) of 10%, a small portion of the world's largest rivers already have an installed storage capacity that puts river's ability to provide environmental services at risks. With increasing environmental flow guidelines, more river basins would be considered "overdeveloped" even with current storage capacity. This shows that existing reservoirs are partially causing the deterioration of ecosystem services, and reservoir storage potential would be further constrained by more stringent environmental flow requirements.

4. Discussions and conclusions

This paper quantified the global potential for surface water reservoirs to provide a firm yield across four different climate change scenarios and two socioeconomic development pathways under a maximum reservoir expansion scenario. Competing land-use activities are found to pose a nontrivial impact on reservoir storage potential worldwide. Approximately 4-13% of the estimated maximum storage capacity is unavailable due to human occupation, existing irrigated cropland, and protected areas. In addition, net evaporation is non-trivial (~2.3% of total annual firm yield) and it is anticipated to increase ~3-4% under the most extreme climate warming scenario (RCP8.5). Importantly, the impact of climate change on reservoirs differs immensely from basin-to-basin, but the results of this analysis show agreement in terms of its negative role in reservoir reliability. International policies aimed at reducing greenhouse gas emissions would help to reduce this uncertainty, and therefore point to additional co-benefits of climate change mitigation in terms of improving long-term water supply reliability.

Two types of bivariate map products were generated from this study to help decision makers understand the potential benefits of reservoir expansion at the basin-scale and help define regional adaptation measures needed for water security. By linking this framework with anthropogenic water demand for various activities in each basin (e.g., agriculture, electricity, industry, domestic, manufacturing, mining, livestock), regions where water is severely in deficit, and thus, expanding reservoirs would potentially relieve regional water scarcity could be identified. Other than demand for water, alternative metrics that could presumably affect reservoir expansions include, but are not limited to, economic incentives, institutional capacity, and infrastructure readiness.

This paper should not be seen as a call for more large dams, but rather an assessment of where policies and infrastructure investments are needed to sustain and improve global water security. In fact, dam removal activities have become more prominent in the United States since the 2000s, partly due to concerns of deteriorating river ecosystems and degraded environmental services (Oliver, 2017). A recent study by the Mekong River Commission tested a scenario of completing 78 dams on the tributaries between 2015-2030, the results of which suggested that it would have catastrophic impacts on fish productivity and biodiversity (Ziv et al., 2011). Therefore, it is critical to consider the trade-offs between socioeconomic progress and sustainable development when interpreting results with the tools built from this study.

This study serves as a valuable input to future work connecting water, energy, land and socioeconomic systems into a holistic assessment framework. Future effort will include other metrics described above to further constrain reservoir storage potential. Future work could also examine sensitivity of the results to a wider range of GHMs and GCMs to better capture model uncertainty. Finally, the results of this study provide planners with important quantitative metrics for long-term water resource planning and help explore the implications through integrated modeling of water sector development.

Acknowledgements

Part of this research was developed during the Young Scientists Summer Program at the International Institute for Applied Systems Analysis (IIASA), with financial support from the

IIASA Annual Fund. The authors acknowledge the Global Environment Facility (GEF) for funding the development of this research as a part of the "Integrated Solutions for Water, Energy, and Land (ISWEL)" project (GEF Contract Agreement: 6993), and the support of the United Nations Industrial Development Organization (UNIDO). We also acknowledge the Coupled Model Intercomparison Project Phase 5 (CMIP5) and the Inter-Sectoral Impact Model Intercomparison Project (ISI-MIP) for providing the climate and hydrological data. We also thank Nils Johnson for his input during the early formulations of this research.

References

ASAE, 1993. Heating, Ventilating and Cooling Greenhouses. American Society of Agricultural Engineers, St. Joseph, MI 49085.

Boehlert, B., Solomon, S., Strzepek, K.M., 2015. Water under a changing and uncertain climate: Lessons from climate model ensembles. J. Clim. 28, 9561–9582. doi:10.1175/JCLI-D-14-00793.1

Budyko, M.I., Milelr, D.H., 1974. Methods for Determining the Components of the Heat Balance, in: Climate and Life. Academic Press, New York.

Carty, J.G., Cunnane, C., 1990. An evaluation of some methods for determining storage yield relationships for impounding reservoirs. J. IWEM 53, 570–572.

de Vries, B.J.M., van Vuuren, D.P., Hoogwijk, M.M., 2007. Renewable energy sources: Their global potential for the first-half of the 21st century at a global level: An integrated approach. Energy Policy 35, 2590–2610. doi:10.1016/j.enpol.2006.09.002

Deguignet, M., Juffe-Bignoli, D., Harrison, J., Macsharry, B., Burgess, N., Kingston, N., 2014. 2014 United Nations list of Protected Areas, UNEP-WCMC : cambrige, UK.

Fricko, O., Parkinson, S., Johnson, N., Strubegger, M., Vliet, M.T. van, Riahi, K., 2016. Energy sector water use implications of a 2°C climate policy Oliver. Environ. Res. Lett. 11. doi:10.1088/1748-9326/11/3/034011

Gaupp, F., Hall, J., Dadson, S., 2015. The role of storage capacity in coping with intra-annual runoff variability on a global scale. Environ. Res. Lett. 17, 3943. doi:10.1088/1748-9326/10/12/125001

Grubert, E.A., 2016. Water consumption from hydroelectricity in the United States. Adv. Water Resour. 96, 88–94. doi:10.1016/j.advwatres.2016.07.004

Harwell, G.R., 2012. Estimation of evaporation from open water—A review of selected studies, summary of U.S. Army Corps of Engineers data collection and methods, and evaluation of two methods for estimation of evaporation from five reservoirs in Texas, U.S. Geological Survey Scientific Investigations Report 2012–5202.

Hempel, S., Frieler, K., Warszawski, L., Schewe, J., Piontek, F., 2013. A trend-preserving bias correction – the ISI-MIP approach. Earth Syst. Dynam. 4, 219–236. doi:10.5194/esd-4-219-2013

Jones, B., Neill, B.C.O., Hegre, H., Buhaug, H., Calvin, K. V, Wiebe, K., Lotze-campen, H., Sands, R., Müller, C., Elliott, J., Chryssanthacopoulos, J., 2016. Spatially explicit global population scenarios consistent with the Shared Socioeconomic Pathways. Environ. Res. Lett. 11. doi:doi:10.1088/1748-9326/11/8/084003

Jones, C.D., Hughes, J.K., Bellouin, N., Hardiman, S.C., Jones, G.S., Knight, J., Liddicoat, S., O’Connor, F.M., Andres, R.J., Bell, C., Boo, K.O., Bozzo, A., Butchart, N., Cadule, P., Corbin, K.D., Doutriaux-Boucher, M., Friedlingstein, P., Gornall, J., Gray, L., Halloran, P.R., Hurtt, G., Ingram, W.J., Lamarque, J.F., Law, R.M., Meinshausen, M., Osprey, S., Palin, E.J., Parsons Chini, L., Raddatz, T., Sanderson, M.G., Sellar, A.A., Schurer, A., Valdes, P., Wood, N., Woodward, S., Yoshioka, M., Zerroukat, M., 2011. The HadGEM2-ES implementation of CMIP5 centennial simulations. Geosci. Model Dev. 4, 543–570. doi:10.5194/gmd-4-543-2011

Kundzewicz, Z.W., Stakhiv, E.Z., 2010. Are climate models “ready for prime time” in water resources management applications, or is more research needed? Hydrol. Sci. J. 55, 1085–1089. doi:10.1080/02626667.2010.513211

Kuria, F.W., Vogel, R.M., 2015. Global Storage-Reliability-Yield Relationships for Water Supply Reservoirs. Water Resour. Manag. 29, 1591–1605. doi:10.1007/s11269-014-0896-4

Lehner, B., Liermann, C.R., Revenga, C., Vörösmarty, C., Fekete, B., Crouzet, P., Döll, P., Endejan, M., Frenken, K., Magome, J., Nilsson, C., Robertson, J.C., Rödel, R., Sindorf, N., Wisser, D., 2011. High-resolution mapping of the world's reservoirs and dams for sustainable river-flow management. Front. Ecol. Environ. 9, 494–502. doi:10.1890/100125

Lele, S.M., 1987. Improved algorithms for reservoir capacity calculation incorporating storage???dependent losses and reliability norm. Water Resour. Res. 23, 1819–1823. doi:10.1029/WR023i010p01819

McDonald, R.I., Weber, K., Padowski, J., Flörke, M., Schneider, C., Green, P.A., Gleeson, T., Eckman, S., Lehner, B., Balk, D., Boucher, T., Grill, G., Montgomery, M., 2014. Water on an urban planet: Urbanization and the reach of urban water infrastructure. Glob. Environ. Chang. 27, 96–105. doi:10.1016/j.gloenvcha.2014.04.022

McMahon, T.A., Vogel, R.M., Pegram, G.G.S., Peel, M.C., Etkin, D., 2007. Global streamflows - Part 2: Reservoir storage-yield performance. J. Hydrol. 347, 260–271. doi:10.1016/j.jhydrol.2007.09.021

Merva, G.E., 1975. Physio Engineering Principles. West Port AVI Publishing Co.

Naden, P.S., 1992. Spatial variability in flood estimation for large catchments: the exploitation of channel network structure. Hydrol. Sci. J. 37, 53–71. doi:10.1080/02626669209492561

O'Neill, B.C., Kriegler, E., Ebi, K.L., Kemp-Benedict, E., Riahi, K., Rothman, D.S., van Ruijven, B.J., van Vuuren, D.P., Birkmann, J., Kok, K., Levy, M., Solecki, W., 2014. The roads ahead: Narratives for shared socioeconomic pathways describing world futures in the 21st century. Glob. Environ. Chang. doi:10.1016/j.gloenvcha.2015.01.004

Oliver, M., 2017. Liberated Rivers: Lessons from 40 years of dam removal. PNW Sci. Find. 1–4.

Penman, H.L., 1948. Natural evaporation from open water, bare soil and grass. Proc. R. Soc. London. Ser. A. Math. Phys. Sci. 193, 120 LP-145.

Poff, N.L., Schmidt, J.C., 2016. How dams can go with the flow. Science (80-.). 353, 1099 LP-1100.

Riahi, K., Rao, S., Krey, V., Cho, C., Chirkov, V., Fischer, G., Kindermann, G., Nakicenovic, N., Rafaj, P., 2011. RCP 8.5-A scenario of comparatively high greenhouse gas emissions. Clim. Change 109, 33–57. doi:10.1007/s10584-011-0149-y

Richter, B.D., Davis, M.M., Knorad, C., 2012. A presumptive standard for environmental flow protection. River Res. Appl. 28, 1312–1321. doi:10.1002/rra.1511

Richter, B.D., Postel, S., Revenga, C., Lehner, B., Churchill, A., 2010. Lost in Development ' s Shadow : The Downstream Human Consequences of Dams. Water Altern. 3, 14–42.

Rippl, W., 1883. The capacity of storage-reservoirs for water supply. Minutes Proc. Inst. Civ. Eng. 71, 270–278.

Schewe, J., Heinke, J., Gerten, D., Haddeland, I., Arnell, N.W., Clark, D.B., Dankers, R., Eisner, S., Fekete, B.M., Colón-González, F.J., Gosling, S.N., Kim, H., Liu, X., Masaki, Y., Portmann, F.T., Satoh, Y., Stacke, T., Tang, Q., Wada, Y., Wisser, D., Albrecht, T., Frieler, K., Piontek, F., Warszawski, L., Kabat, P., 2014. Multimodel assessment of water scarcity under climate change. Proc. Natl. Acad. Sci. U. S. A. 111, 3245–3250. doi:10.1073/pnas.1222460110

Shuttleworth, W.J., 1993. Evaporation, in: Maidment, D.R. (Ed.), Handbook of Hydrology, Civil Engineering. McGraw-Hill.

Siebert, S., Henrich, V., Frenken, K., Burke, J., 2013. Global Map of Irrigation Areas version 5.

Soundharajan, B.S., Adeloye, A.J., Remesan, R., 2016. Evaluating the variability in surface water reservoir planning characteristics during climate change impacts assessment. J. Hydrol. 538, 625–639. doi:10.1016/j.jhydrol.2016.04.051

Stillwell, A.S., Webber, M.E., 2013. Evaluation of power generation operations in response to changes in surface water reservoir storage. Environ. Res. Lett. 8, 25014. doi:10.1088/1748-9326/8/2/025014

Tennant, D.L., 1976. Instream flow regimens for fish, wildlife, recreation, and related environmental resources, in Instream flow needs， Volume II: Boise, ID, in: Proceedings of the Symposium and Specialty Conference on Instream Flow Needs. pp. 359–373.

Turner, S.W.D., Galelli, S., 2016. Water supply sensitivity to climate change: An R package for implementing reservoir storage analysis in global and regional impact studies. Environ. Model. Softw. 76, 13–19. doi:10.1016/j.envsoft.2015.11.007

van Beek, L.P.H., Eikelboom, T., van Vliet, M.T.H., Bierkens, M.F.P., 2012. A physically based model of global freshwater surface temperature. Water Resour. Res. 48. doi:10.1029/2012WR011819

van Beek, L.P.H., Wada, Y., Bierkens, M.F.P., 2011. Global monthly water stress: 1. Water balance and water availability. Water Resour. Res. 47. doi:10.1029/2010WR009791

van Vliet, M.T.H., van Beek, L.P.H., Eisner, S., Flörke, M., Wada, Y., Bierkens, M.F.P., 2016. Multi-model assessment of global hydropower and cooling water discharge potential under climate change. Glob. Environ. Chang. 40, 156–170. doi:http://dx.doi.org/10.1016/j.gloenvcha.2016.07.007

van Vuuren, D.P., Edmonds, J., Kainuma, M., Riahi, K., Thomson, A., Hibbard, K., Hurtt, G.C., Kram, T., Krey, V., Lamarque, J.F., Masui, T., Meinshausen, M., Nakicenovic, N., Smith, S.J., Rose, S.K., 2011. The representative concentration pathways: An overview. Clim. Change 109, 5–31. doi:10.1007/s10584-011-0148-z

Veldkamp, T.I.E., Wada, Y., Aerts, J.C.J.H., Ward, P.J., 2016. Towards a global water scarcity risk assessment framework: incorporation of probability distributions and hydro-climatic variability. Environ. Res. Lett. 11, 24006.

Vogel, R.M., Sieber, J., Archfield, S.A., Smith, M.P., Apse, C.D., Huber-Lee, A., 2007. Relations among storage, yield, and instream flow. Water Resour. Res. 43, 1–12. doi:10.1029/2006WR005226

Vogel, R.M., Stedinger, J.R., 1987. Generalized storage-reliability-yield relationships. J. Hydrol. 89, 303–327. doi:10.1016/0022-1694(87)90184-3

Vörösmarty, C.J., Vo, C.J., Green, P., 2009. Global Water Resources : Vulnerability from Climate Change and Population Growth. Science (80-.). 284. doi:10.1126/science.289.5477.284

Wada, Y., Lo, M.-H., Yeh, P.J.-F., Reager, J.T., Famiglietti, J.S., Wu, R.-J., Tseng, Y.-H., 2016. Fate of water pumped from underground and contributions to sea-level rise. Nat. Clim. Chang. IN PRESS, 8–13. doi:10.1038/nclimate3001

Wada, Y., Wisser, D., Bierkens, M.F.P., 2014. Global modeling of withdrawal, allocation and consumptive use of surface water and groundwater resources. Earth Syst. Dyn. 5, 15–40. doi:10.5194/esd-5-15-2014

Wanders, N., Wada, Y., Van Lanen, H.A.J., 2015. Global hydrological droughts in the 21st century under a changing hydrological regime. Earth Syst. Dynam. 6, 1–15. doi:10.5194/esd-6-1-2015

Wee, S.L., 2012. Thousands being moved from China's Three Gorges - again [WWW Document]. Reuters. URL http://www.reuters.com/article/us-china-threegorges-idUSBRE87L0ZW20120822 (accessed 1.1.16).

Wiberg, D., Strzepek, K.M., 2005. Development of Regional Economic Supply Curves for Surface Water Resources and Climate Change Assessments : A Case Study of China. Laxenburg, Austria.

Young, G.K., Puentes, C.D., 1969. Storage yield: Extending the Sequent Peak Algorithm to multiple reservoirs. Water Resour. Res. 5, 1110–1114. doi:10.1029/WR005i005p01110

Zhou, Y., Hejazi, M., Smith, S., Edmonds, J., Li, H., Clarke, L., Calvin, K., Thomson, A., 2015. A comprehensive view of global potential for hydro-generated electricity. Energy Environ. Sci. 8, 2622–2633. doi:10.1039/C5EE00888C

Ziv, G., Baran, E., Nam, S., Rodríguez-Iturbe, I., Levin, S.A., 2011. Trading-offfish biodiversity, food security, and hydropower in the Mekong River Basin 109, 5609–5614. doi:10.1073/pnas.1201423109

Appendix A

1. Simplified area-volume relationship for reservoirs

A nonlinear area (A)-volume (V) relationship is identified in the form of

$$V = cA^b \tag{4}$$

where c and b are basin-specific parameters. The area-volume relationship is derived from GRanD data of existing reservoirs within each basin. In basins where no reservoirs currently exist, a uniform relationship is derived from all reservoirs globally. c_{max} in equation 3g is calculated for each basin by plugging in estimated total available land area as discussed in section 2.3.

Based on GRanD data for existing reservoirs, we further provided an estimate of the a variable in equation (2). We simply took the ratio of the sum of surface area and the sum of maximum storage capacity for all existing reservoirs within each basin, and assume this ratio to be the surface area per unit storage volume (a) for each representative reservoir.

The area-volume relationships extrapolated from the GRanD database reflect some level of topographic features of the region but lack explicit characterization of the terrain at sufficient resolutions needed to site specific locations for new reservoirs. However, the basin-averaged relationships capture the main topographic variations across regions, and given the global scale of this study, this simplification is considered an acceptable first-order approximation.

2. Net evaporation calculation

Storing water in reservoirs increases the surface area of the waterbody, which results in increased evaporation. Net evaporative losses from the reservoir surface were computed on a 0.5-degree global grid for each RCP scenario. First, the evaporation (mm/day) from the aggregated reservoir surface is estimated using the method developed by Shuttleworth (1993) as

$$e_e = \frac{mR_n + \gamma \times 6.43 \times (1 + 0.536 \times U_s)\delta_e}{\lambda_v(m + \gamma)} \quad (5)$$

where e_e is the estimated evaporation in mm day^{-1}, U_s is the wind speed in m s^{-1}, and λ_v is the latent heat of vaporization of water in MJ kg^{-1}. The model parameter δ_e is the vapor pressure deficit in kPa, and is computed from

$$\delta_e = (1 - RH)e_s \quad (6)$$

where RH is relative humidity in % and e_s is saturated vapor pressure in kPa, which can be obtained using the approximation in *Merva* (1975). R_n is net irradiance in MJ m^{-2} day^{-1}, which is computed as

$$R_n = (1 - \alpha)R_{SW}^{\downarrow} + R_{LW}^{\downarrow} - \varepsilon\sigma T_s^4 \quad (7)$$

where α is the albedo of water (assumed to be 0.1, adopted from Table 8 in Budyko and Milelr, 1974), $R_{SW}^{\downarrow}$ is downward shortwave radiation and $R_{LW}^{\downarrow}$ is downward longwave radiation in MJ m^{-2} day^{-1}. ε is the broad band emissivity of water (assumed to be 0.96 as a mid-value in the cited range (http://www.engineeringtoolbox.com/emissivity-coefficients-d_447.html)), σ is the Stephan-Boltzmann constant (5.67×10^{-8} kg s^{-3} K^{-4}), and T_s is the surface temperature of water in K. The psychrometric constant γ in kPa K^{-1} is estimated as

$$\gamma = \frac{0.0016286P}{\lambda_v} \tag{8}$$

where P is surface atmospheric pressure in kPa. The last variable m is defined as the slope of the saturation vapor pressure curve in kPa K^{-1}, which is estimated following *ASAE* (1993) as

$$m = \frac{de_s}{dT_a} = 0.04145e^{0.06088\,(T_a - 273.15)} \tag{9}$$

where T_a is the surface air temperature in K. Net evaporation e (mm/day) is therefore the difference between estimated evaporation e_s and precipitation p (mm/day).

$$e = e_e - p \tag{10}$$

Basin-specific total net evaporation in volumetric units (m^3) is obtained by multiplying the basin averaged net evaporation rate by total aggregated reservoir surface area (A_t in equation (2)) within each basin.

3. Exclusion zones

Table S1 lists important characteristics of the datasets used to define the three exclusion zones in this study.

Table S1 Summary of data that defines the exclusion zones

Exclusion zones	**Source**	**Data versions**	**Unit**	**Resolution**	**Varies over time?**
Population	Jones et al., 2016	SSP1, SSP2, SSP3, SSP4, SSP5	Number of people	0.125 degree	Yes
Irrigated Cropland	Siebert et al., 2013	Irrigated and rain-fed	Percentage of area per grid cell	0.0833 degree	Static
Protected area	Deguignet et al., 2014	World Database on Protected Areas (WDPA)	Locations of protected area (land and marine)	Polygons	Static

Protected land and irrigated cropland area are held constant over the simulation horizon due to a lack of suitable projections aligned with the SSP scenarios. It is important to note that future expansion of irrigated cropland is anticipated and could further restrict reservoir expansion. Developing specific rules and policies reflecting siting decisions, as well as policies addressing future protected areas, is beyond the scope of this current study. Grid cells occupied by urban population, existing irrigated cropland, or designated as a protected area are considered as exclusion zones. These exclusion zones occupy about 70 million km^2 of areal coverage, which is about 46% of Earth's total land area. Historical reservoir development suggests that areas occupied by rural population are considered potentially available lands for reservoir expansion (Richter et al., 2010; Ziv et al., 2011). There is significant controversy surrounding the ethics of flooding upstream populated areas for reservoir development, and as engineering scientists we decided to approach this issue by defining a range of rural population density cutoff values above which grid-cells are considered unfit for reservoir expansion. Essentially, a cutoff value of rural population density equal to 0 capita per km^2 suggests that all rural areas are considered un-exploitable for reservoir expansion; a cutoff value of 1244 capita per km^2, which is obtained from the number of rural residents relocated for building the Three Gorges Dam (Wee, 2012), is assumed in this study to be a maximum limit for relocation of rural populations due to reservoir inundation. A higher threshold suggests more land for reservoirs and less land to be retained for rural population.

4. Impact of exclusion zones

We examined the impact of exclusion zones on reservoir storage potential for each basin by applying a sensitivity analysis where the following parameters are varied: 1) cutoff value for rural population density, below which grids cells are available for reservoir expansions, and 2) total population growth trajectory. The cutoff value is hypothetically assumed except for the maximum cutoff value in this sensitivity analysis (Appendix A section 3). Parameter 1) and 2) will vary the total available land for reservoir expansion, and hence, the c_{max} variable in equation 3g.

Figure S5 shows the impact of exclusion zones on global reservoir storage potential while incorporating the sensitivity analysis on the cutoff value for rural population relocation. Overall, ~4% of reservoir storage potential would be unavailable because of pre-existing land occupations by irrigated cropland, protected land and urbanization, regardless of the differences in rural density cutoff value and population development. Impacts on global reservoir storage potential also show an overall increasing trend over time, which corresponds to the decreasing available land due to increasing population trajectories under the two SSPs. Looking across different cutoff values for rural popilation, impacts on reservoir storage potential decrease with increasing cutoff value. This is because with a higher cutoff value, more grid cells become available for reservoir expansion, hence, reservoir storage potential is less constrained by land availability. SSP1 describes a future world with high urbanization and low population growth, hence, there is more flexibility to relocate rural population. SSP1 results are more sensitive compared to results from SSP3, which depicts a world with lower urbanization and higher population growth, and therefore is less flexible toward vacating highly-populated rural lands. Therefore, exclusion zones have important implications on the amount of global reservoir storage potential.

Overall, global maximum storage capacity is estimated to be ~5 times the current capacity volume (~6197 km^3). However, due to exclusion zone constraints, the reservoir storage potential is about 87-96% of the estimated maximum storage capacity, which suggest that the exploitable storage capacity is ~4.3-4.8 times the current storage capacity.

5. Impact of climate change

Climate change impacts vary substantially from basin to basin (Figure S6) which highlights the significant geographical variability in terms of climate change impacts on hydrologic processes. Figure S6a shows the effect of climate change on the basin averaged net evaporative loss at a global scale under four different RCPs. On average, the net evaporation loss accounts for ~2.3% of the total annual firm yield. Differences among RCPs are minimal because the increases and decreases, in general, balance out when aggregated to the global-scale. However, there is a discernible difference in the trend of net evaporative loss over time, particularly for RCP8.5, which shows ~3.7% of net evaporative loss by the 2080s. The range of differences between basins (extent of box in Figure S6a) is expected to widen over time with climate change, indicating the importance of quantifying and understanding the spatial variability of net evaporative losses at the basin scale. Climate change mitigation is found to reduce the impacts of reservoir net evaporative loss at the global scale as nearly all basins would have <25% of change in net evaporative losses in the 2080s relative to the historical period via RCP2.6 (Figure S6b). As net evaporation from reservoirs is a non-trivial amount of water supply (~3-4%), these results further underscore the importance of exacerbating impacts from climate change in the context of reservoir management.

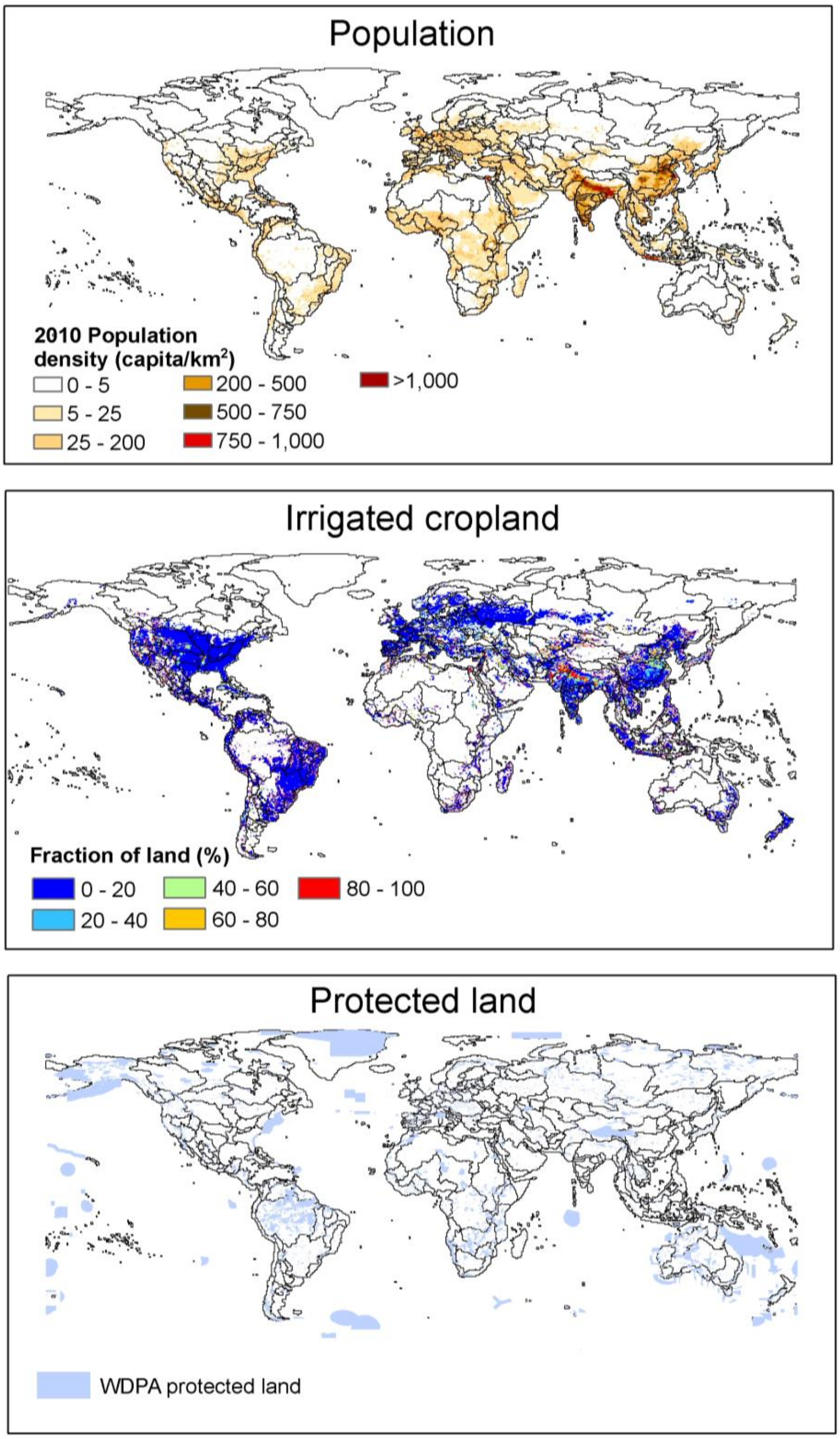

Figure S1. Exclusion zones defined for this study: population (SSP1 projection in 2010 as demonstration), irrigated area, and protected land.

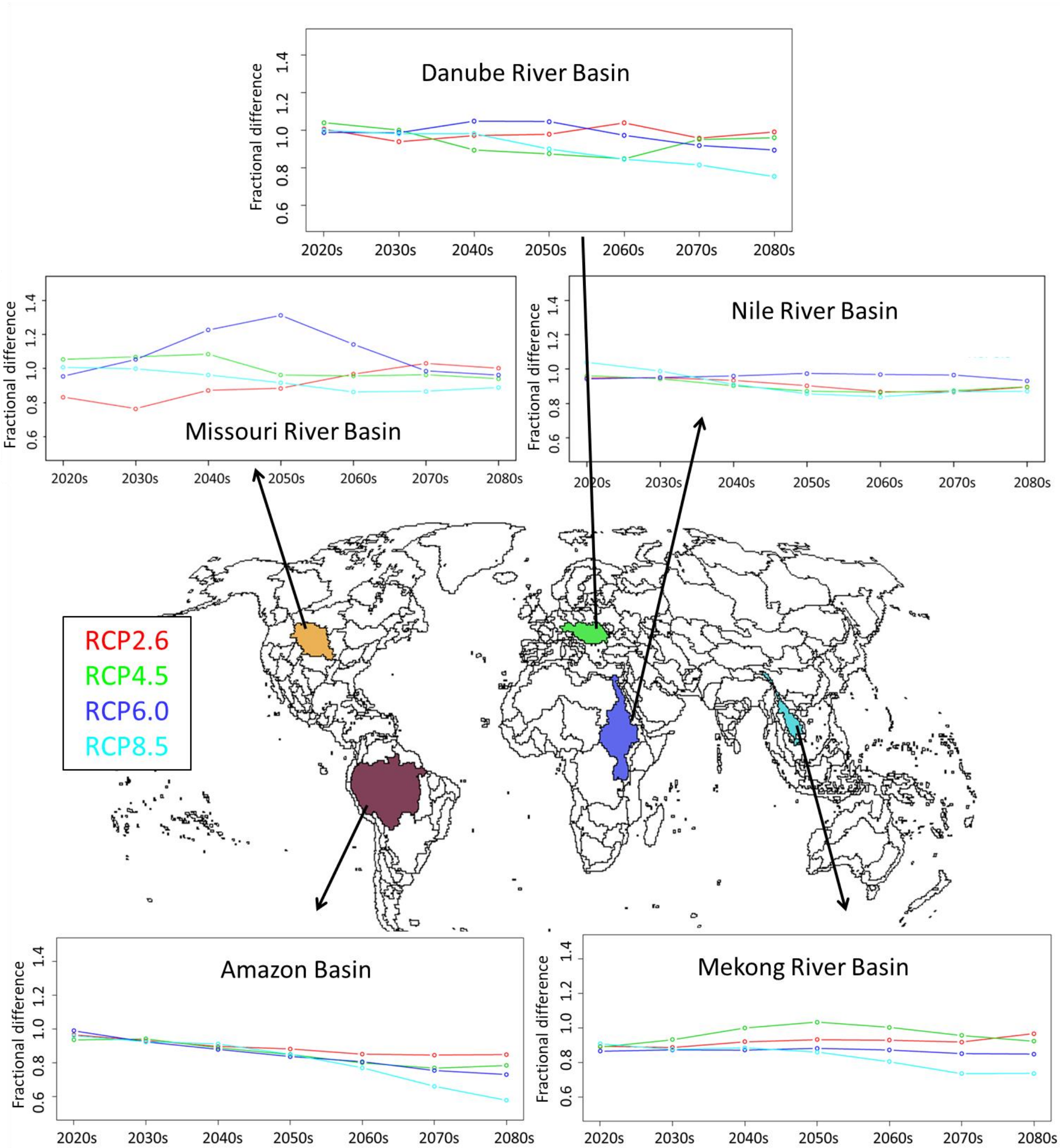

Figure S2. Impacts of climate change on reservoir inflow for selected basins and RCPs. Y-axis values show the fractional difference between the future inflows and the historical inflows.

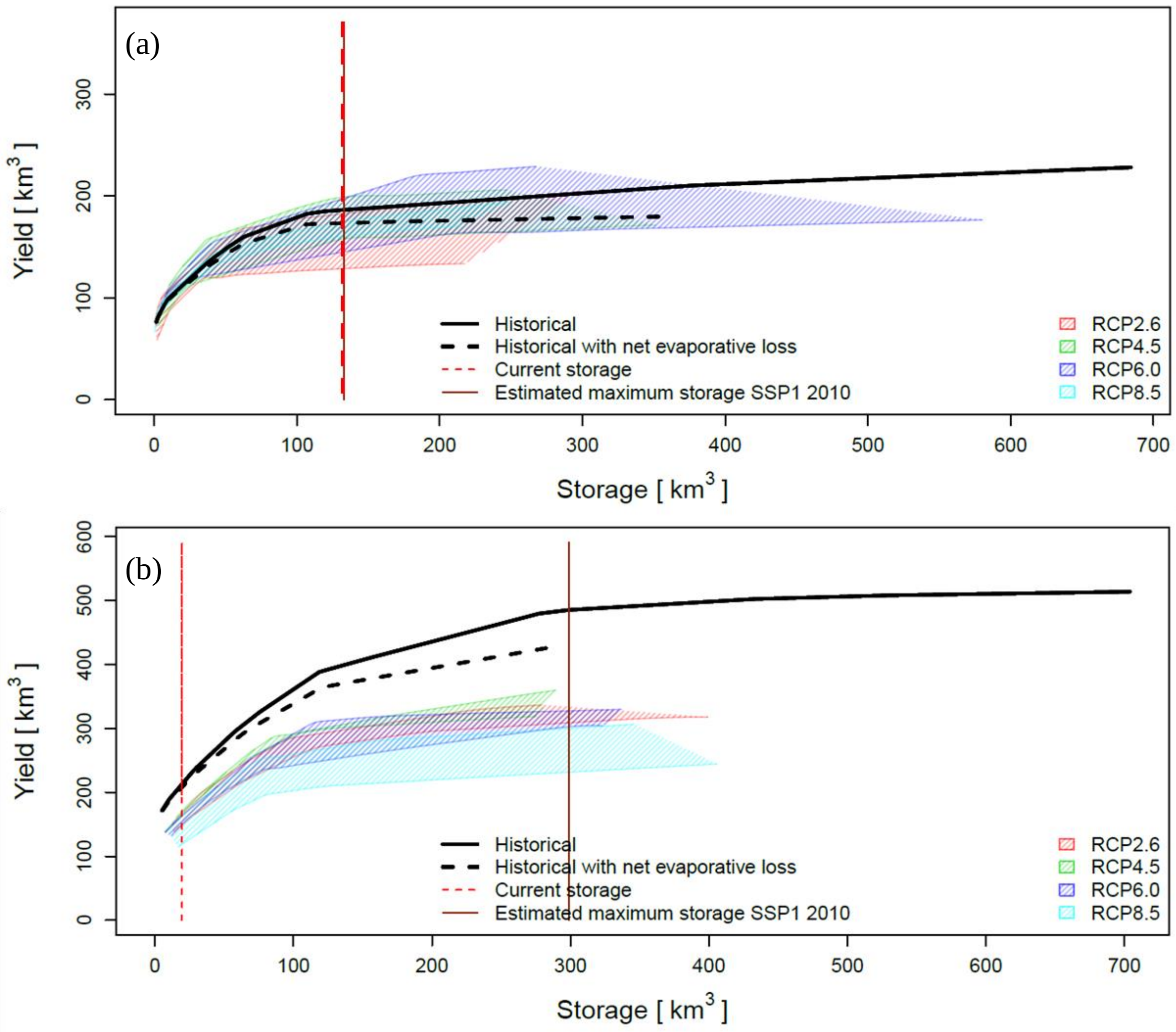

Figure S3. S-Y curve for (a) Missouri River Basin, North America (b) Mekong River Basin, Southeast Asia

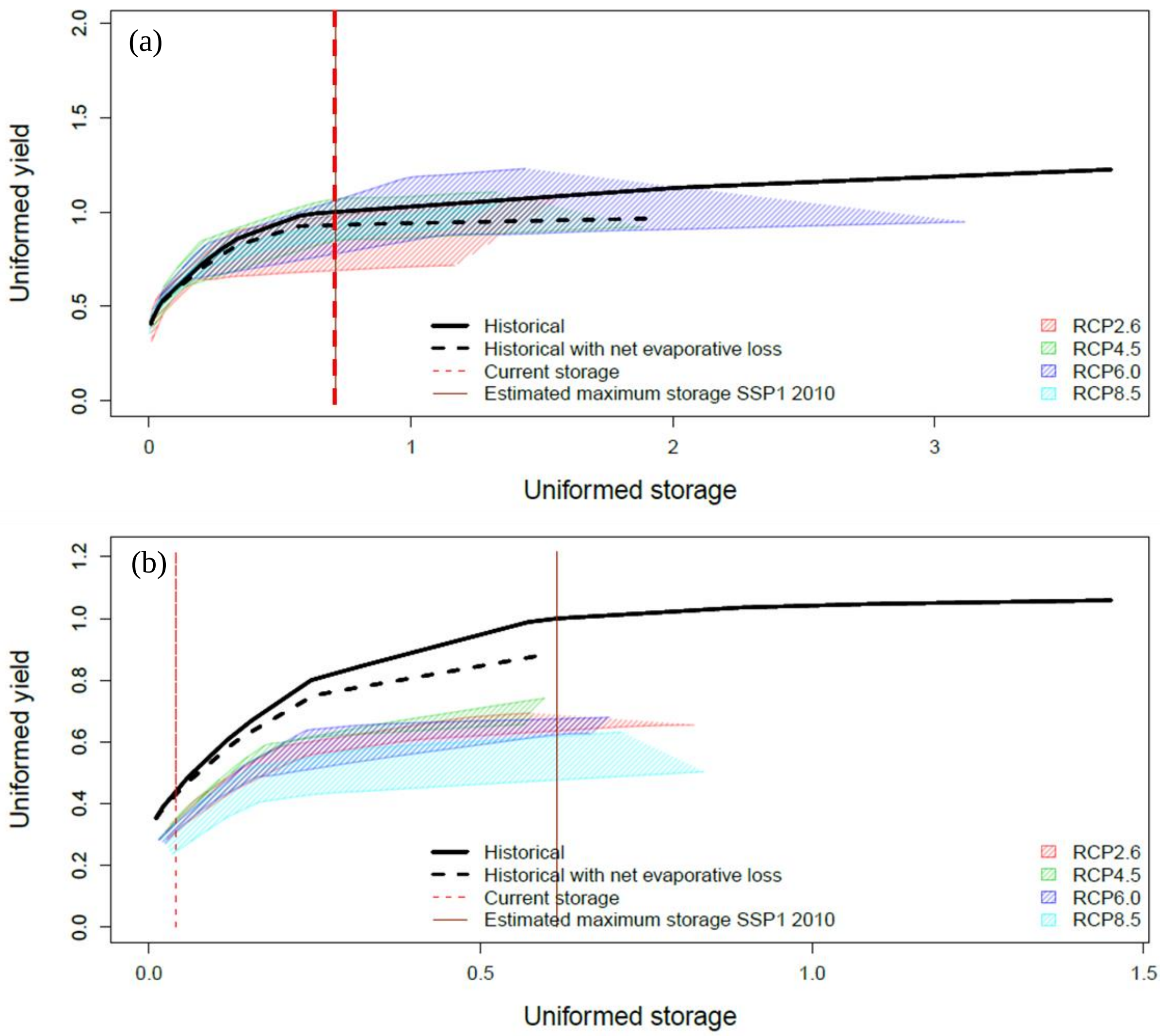

Figure S4. Uniformed S-Y curve for (a) Missouri River Basin, North America (b) Mekong River Basin, Southeast Asia

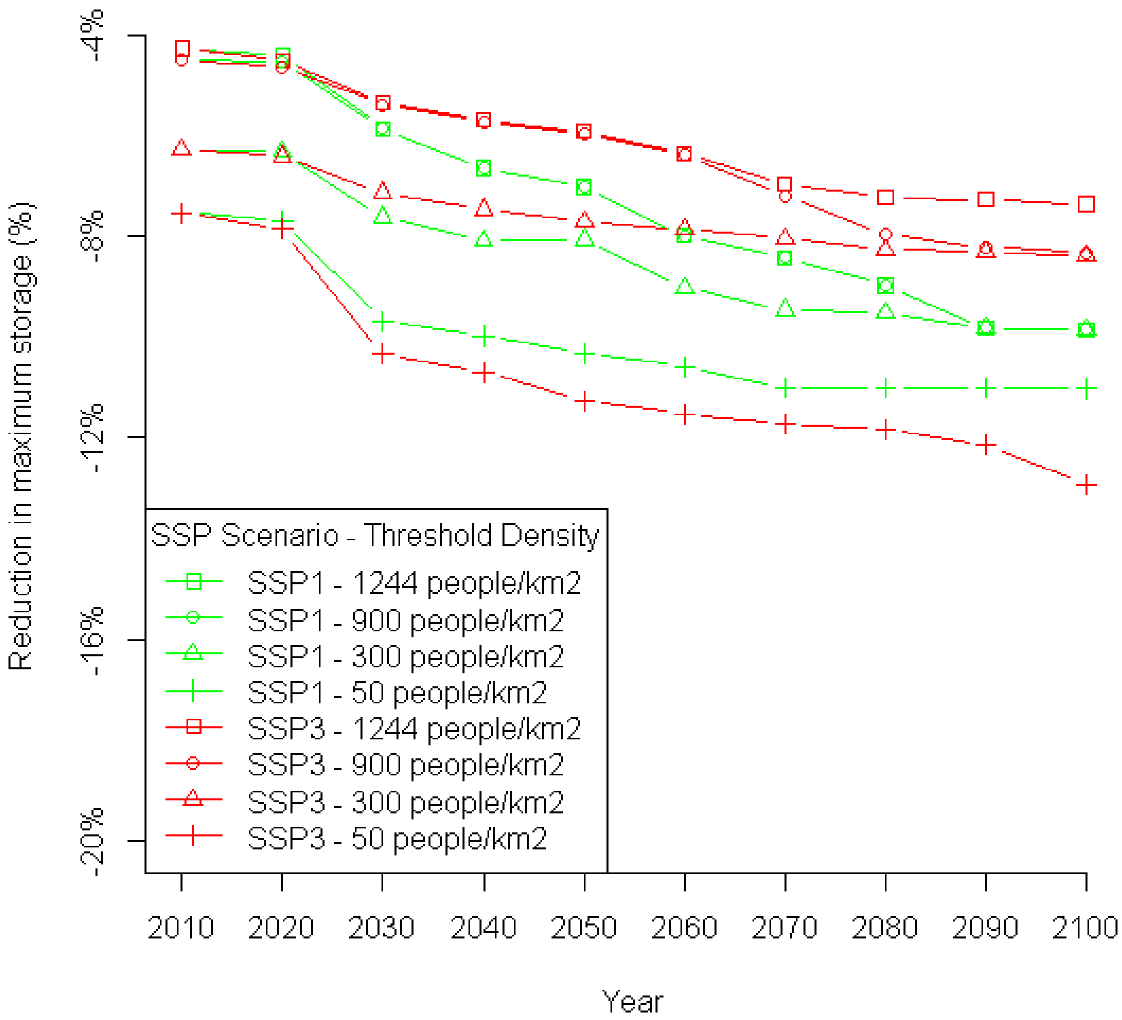

Figure S5. Reduction in global maximum storage capacity due to socioeconomic development under different exclusion zone constraints.

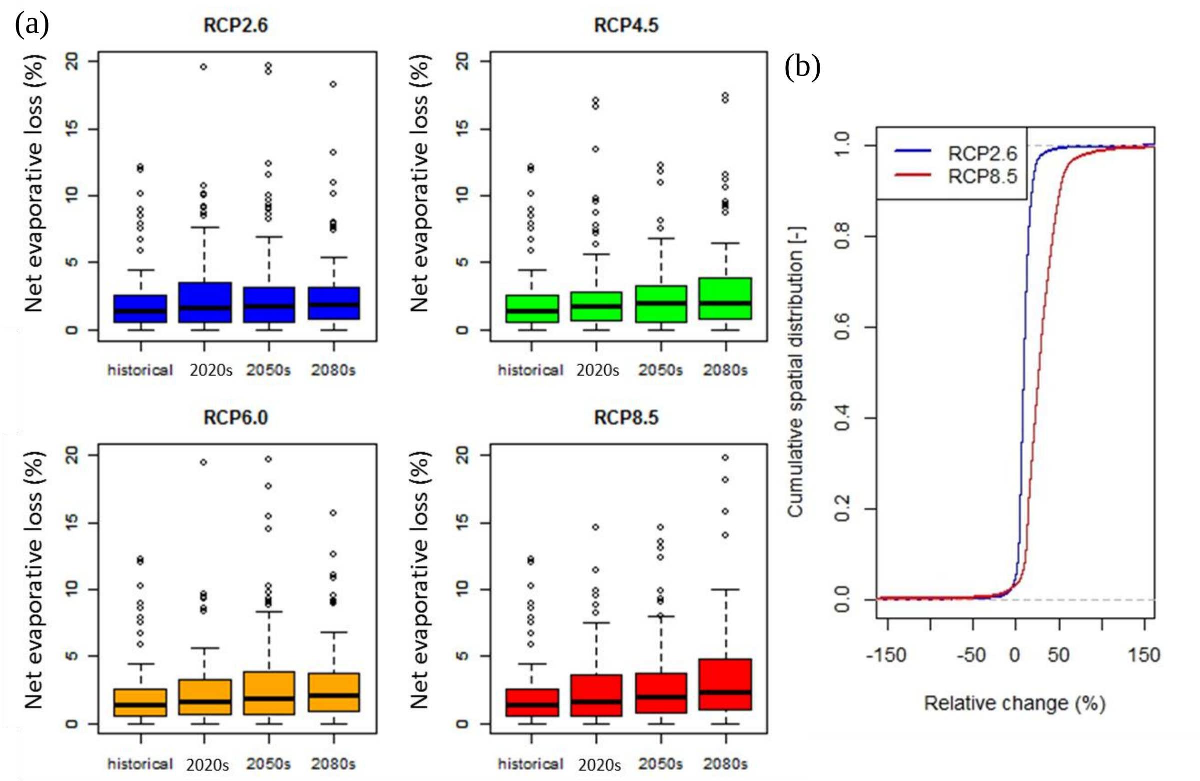

Figure S6. (a) Boxplot of net evaporative loss from basins as percentage of total annual firm yield under four RCPs. The lower- and upper-limits of the box represent the 25th and 75th percentiles, respectively, while the whiskers extend to 1.5 times the interquartile range. The outliers extend to the most extreme outcomes. (b) Cumulative spatial distribution of change of net evaporation in the 2080s relative to the historical period under RCP2.6 and RCP8.5.

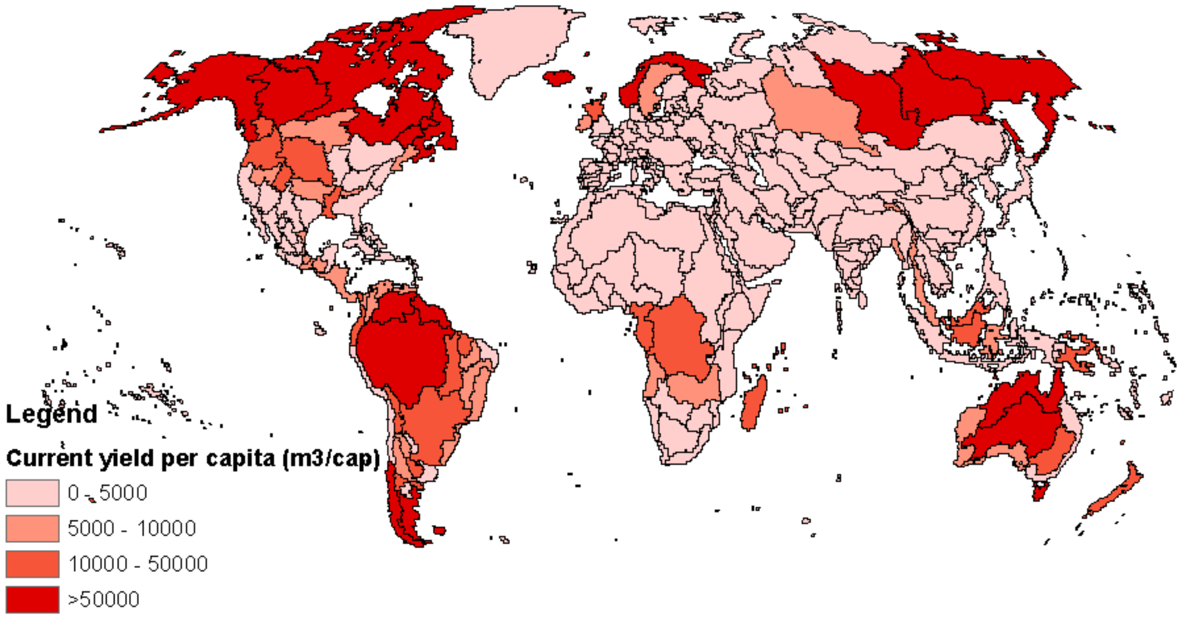

Figure S7. Current yield per capita per basin.

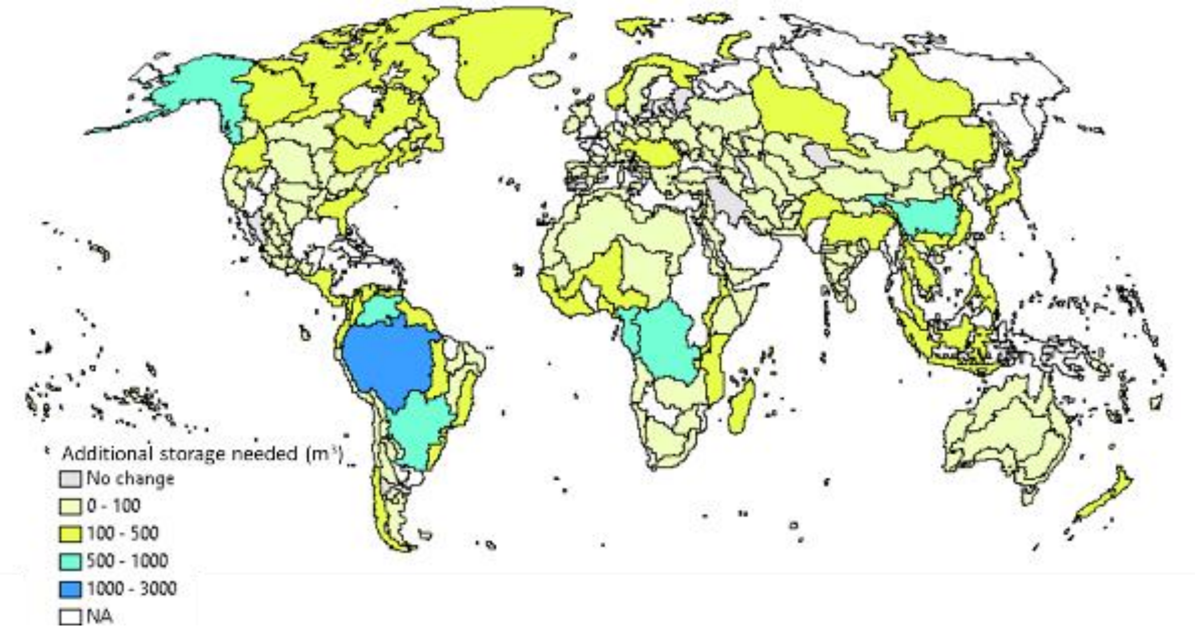

Figure S8. Additional storage capacity needed for maintaining current firm yield (based on RCP2.6 scenario in the 2050s).